Supporting Information

Redox Catalysis Promoted Fast Iodine Kinetics for Polyiodide-Free Na-I_2 Electrochemistry

Hong Zhang,[a,b,c,1] Zhoutai Shang,[a,b,1] Siyuan Gao,[d] Bin Song,[e,*] Wenli Zhang,[f] Ruiguo Cao,[b,c] Shuhong Jiao,[b,c] Yingwen Cheng,[d,*] Qianwang Chen,[a,b,c] and Ke Lu[a,b,*]

[a]Institutes of Physical Science and Information Technology, School of Materials Science and Engineering, Key Laboratory of Structure and Functional Regulation of Hybrid Materials of Ministry of Education, Anhui Graphene Engineering Laboratory, Anhui University, Hefei, Anhui 230601, China. Email: luke@ahu.edu.cn (K.L.)
[b]Hefei National Laboratory for Physical Sciences at the Microscale, Hefei, Anhui 230026, China.
[c]Department of Materials Science & Engineering, University of Science and Technology of China, Hefei, Anhui 230026, China.
[d]Department of Chemistry and Biochemistry, Northern Illinois University, DeKalb, Illinois 60115, United States. Email: ycheng@niu.edu (Y.C.)
[e]Laboratory of Nanoscale Biochemical Analysis, Institute of Functional Nano & Soft Materials (FUNSOM), Collaborative Innovation Center of Suzhou Nano Science and Technology (NANO-CIC), Soochow University, Suzhou, Jiangsu 215123, China. Email: bsong@suda.edu.cn (B.S.)
[f]School of Chemical Engineering and Light Industry, Guangdong University of Technology, Guangzhou, Guangdong 510006, China.
[1]H.Z. and Z.S. contributed equally to this work.

Experimental details

Materials synthesis

Preparation of MnO_2 nanorod: The MnO_2 nanorod was prepared by the modified hydrothermal method.[1] Typically, 0.35 mL concentrated HCl (Fisher Scientific) and 2.028 g $MnSO_4$ (Sigma-Aldrich) were added into 300 mL deionized (DI) water. Then, 100 mL DI water solution that contain 1.264 g of $KMnO_4$ (Sigma-Aldrich) was added to the above solution under stirring and stirred for 2 h. The resultant mixture was transferred into a Teflon-lined stainless steel autoclave and heated at 120 ℃ for 12 h. After hydrothermal, the powder product was washed with DI water and ethanol, then vacuum dried at 60 ℃ for 10 h.

Preparation of hollow polyaniline-polypyrrole-$Na_{0.89}Mn[Fe(CN)_6]_{0.73}$ (Polymer-MnHCF) composite matrix: The MnO_2 powder (400 mg) was added into 200 mL DI water and the metal oxide was used as sacrificial template.[2] The Mn^{4+} acted as oxidant and the reduction of Mn^{4+} to Mn^{2+} initiate the simultaneous interfacial co-polymerization of pyrrole (Sigma-Aldrich, 0.5 mmol) and aniline (Sigma-Aldrich, 1 mmol), the Mn^{2+} ions precipitated with $Fe(CN)_6^{4-}$ ($Na_4Fe(CN)_6$, Sigma-Aldrich, 100 mg) render the formation of $Na_{0.89}Mn[Fe(CN)_6]_{0.73}$ (MnHCF), generating coaxial crosslinked polyaniline-polypyrrole-MnHCF@MnO_2 composite. The chemical composition of the $Na_xMn[Fe(CN)_6]_y$ was determined by an inductively coupled plasma atomic emission spectrometer (ICP-AES). The weight percent of MnHCF in Polymer-MnHCF composite was calculated through ICP-AES measurement and the weight percent of MnHCF was about 11 wt%. As control samples, Polymer@MnO_2, PANi-MnHCF@MnO_2, PPy-MnHCF@MnO_2 and MnHCF@MnO_2 were prepared under the similar conditions. The acid leaching treatment in 0.5 M HCl solution for 20 h, and about 100 ml acid solution was used for 100 mg powder.

Preparation of iodine composite cathode: A facile inside-encapsulation method was used to load iodine on different matrixes.[3] Typically, 500 mg iodine powder was put in water to obtain an iodine supersaturated aqueous solution. 300 mg of different scaffolds were immersed into

the solution and stirring for a certain time (at least 24 h). The iodine was continuous adsorbed on multi-pores of scaffold through the "solution-adsorption" process. The as-prepared composites were dried at 80 °C to remove adsorbed water. The time-dependent iodine mass loading was calculated through division of the mass of adsorbed iodine by the mass of carbon and the weight percent of iodine can be easily controlled by the adsorption time.

Physical characterizations:

X-ray diffraction (XRD) spectra were obtained using a Rigaku Miniflex diffractometer (Rigaku D/MAX-γA, Japan). The SEM and TEM images were acquires using Hitachi 650 electron microscope and JEM-2100F microscope with a Bruker EDS detector, respectively, to investigate the microstructures and morphologies. XPS spectra were performed at an ESCALAB 250 X-ray photoelectron spectrometer. The Raman spectra were collected using LabRAM HR 800 system using 514 nm laser. N_2 adsorption-desorption isotherms were recorded on a Kubo × 1000 instrument at 77 K. UV-Vis analysis was measured using a Shimadzu UV-1800 spectrophotometer.

Electrochemical measurements:

Iodine cathodes were prepared by mixing I_2/matrix composite, CNT and polyvinylidene fluoride (PVDF) binder with a mass ratio of 8:1:1 in N-methyl-2-pyrrolidone (NMP). The well mixed slurry was coated on a piece of carbon paper and the iodine mass loading in the rage of 1.6-2.1 mg cm^{-2}. The iodine cathodes were further dried in an Ar-filled glove box for at least 3 days to remove the absorbed water before assemble battery. 2025-type coin cells were assembled in an argon-filled glove box with Na foil as the anode and glass fiber as the separator. The electrolyte was 1 M $NaClO_4$ in ethylene carbonate (EC) and propylene carbonate (PC) (EC: PC = 1:1 volume ratio). All Cyclic voltammetric (CV) measurements were conducted with a CHI 660e/DH7000 electrochemical workstation. The galvanostatic charge/discharge were conducted on a Neware battery tester with cut-off voltages of 2.0 and 3.9 V. Electrochemical impedance spectra were collected using a Gamry Reference 600 potentiostat in the frequency

range of 100 kHz to 100 mHz and an AC amplitude of 5 mV. All the electrochemical experiments were performed at room temperature. The specific capacity was normalized to the mass of iodine. In-situ Raman cells were assembled as the same with normal coin batteries (CR2016) except that the cathode cap was cut into a small hole (5 mm) and covered with a SiO_2 glass. The iodine cathode was prepared by mixing Polymer-MnHCF/I_2, CNT and polyvinylidene fluoride (PVDF) binder with a mass ratio of 9:1:0.5 in N-methyl-2-pyrrolidone (NMP). The well mixed slurry was coated on a piece of stainless steel mesh and the composite mass loading was about 1.5 mg cm^{-2}. The iodine cathodes were further dried in an Ar-filled glove box for at least 3 days to remove the absorbed water before assemble battery. The measurements were taken with the instrument of confocal Raman microscope (LabRAM HR 800) with excitation at 514 nm.

Assemble of beaker cell:

The beaker cell is assembled in an Ar-filled glovebox by using the Polymer-MnHCF/I_2 or Polymer /I_2 electrode as cathode, carbon paper as current collector, Na foil as anode, and 1 M NaClO4 in EC/PC (1:1 by volume) as electrolyte (3 mL). The active material loading of all cathode electrode is 3 mg and the active area (immersed area) is 0.5 cm^2. Visual confirmation of polyiodide formation/entrapment at specific discharge depths (I: 3.2 V vs Na, II: 2.8 V vs Na, III: 2.0 V vs Na) of initial fully discharge process were recorded.

Supplementary note:

The redox reaction between oxidant and monomer can be expressed by:[2]

(1) $MnO_2 + 4H^+ + 2e^- \rightarrow Mn^{2+} + 2H_2O$ (1.23 V vs. RHE)

(2) $n C_4H_4NH$ or $n C_6H_5NH_2 \rightarrow (C_4H_2NH)_n$ or $(C_6H_4NH)_n + 2nH^+ + 2ne^-$ (~0.7 V vs. RHE)

The higher redox potential of Mn^{4+}/Mn^{2+} than the redox polymerization potential of monomer, indicating the spontaneously interfacial polymerization.

Ion co-precipitation reaction: $Mn^{2+} + xNa^+ + yFe(CN)_6^{4-} \rightarrow Na_xMn[Fe(CN)_6]_y\downarrow$

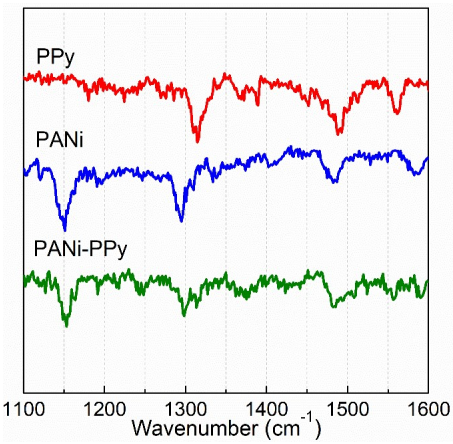

Figure S1: FTIR spectra of pure polyaniline (PANi), polypyrrole (PPy) and cross-linked polyaniline-polypyrrole (PANi-PPy) samples.

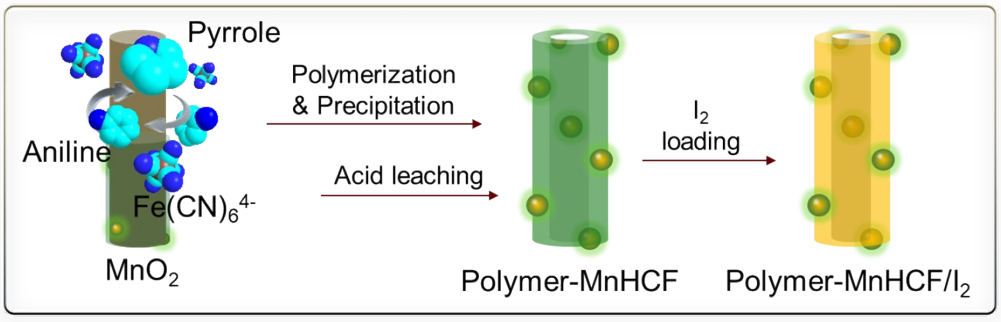

Figure S2: Schematic synthetic route to composite cathode with iodine confined in the multi-pores of Polymer-MnHCF hollow nanorods.

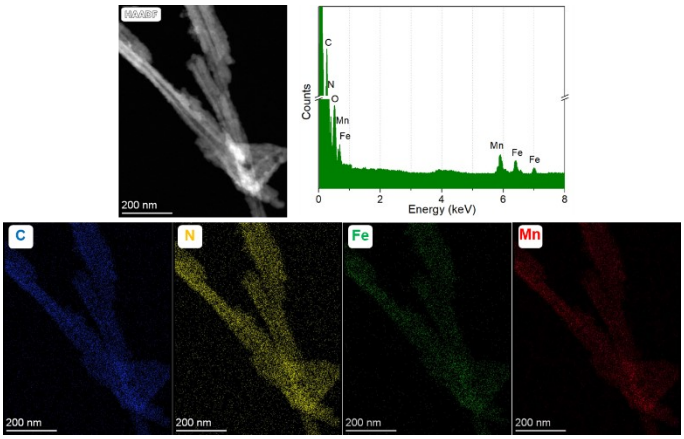

Figure S3: Energy-dispersive X-ray (EDX) spectrum and TEM image and the corresponding elemental mapping of the Polymer-MnHCF matrix.
The energy-dispersive X-ray spectroscopy (EDS) analysis confirms the existence of Mn and Fe elements in the composite matrix. The EDX mapping of Polymer-MnHCF sample confirm Mn, Fe and N were homogeneous distributed. These results could be explained that MnHCF is existed within the polymer framework.

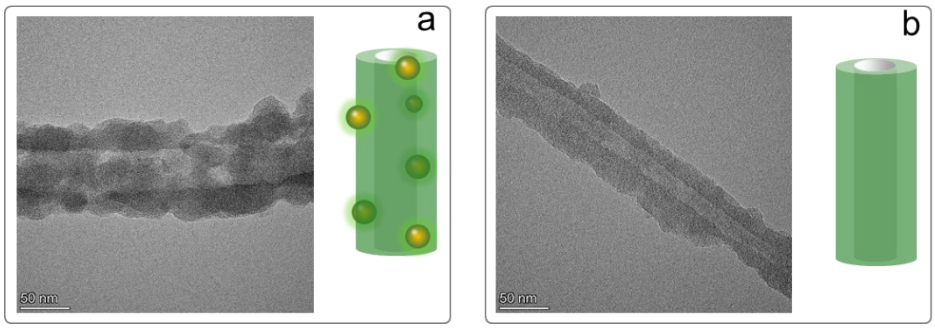

Figure S4: TEM and schematically depicted images of (a) Polymer-MnHCF and (b) Polymer hollow matrixes.

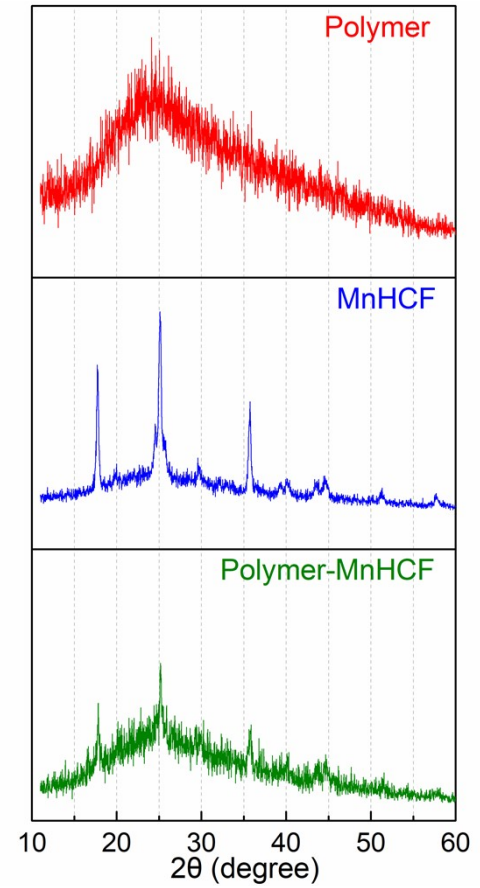

Figure S5: XRD patterns of different materials as noted.

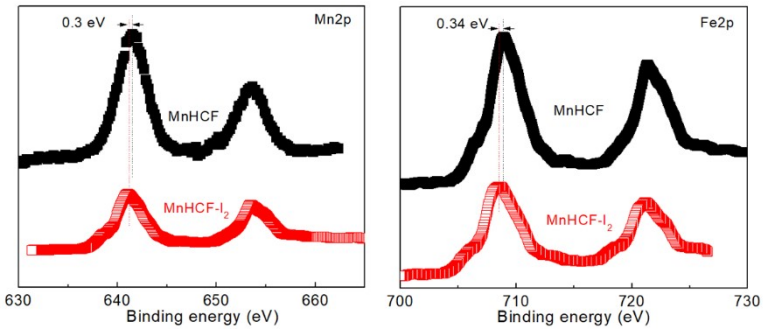

Figure S6: High-resolution XPS spectra of Mn2p and Fe2p for MnHCF and MnHCF-I_2.

After compositing process, the Mn2p and Fe2p spectrum of I_2 adsorbed on MnHCF scaffold shifts about 0.3 eV toward lower binding energy, corresponding to the increase of electron density. The binding energy shift suggests the formation of chemical bonds between substrate and iodine.

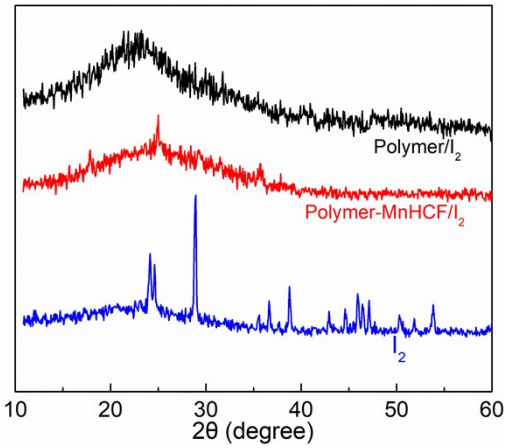

Figure S7: XRD patterns of pure iodine and iodine loaded in different matrixes as composite cathode.

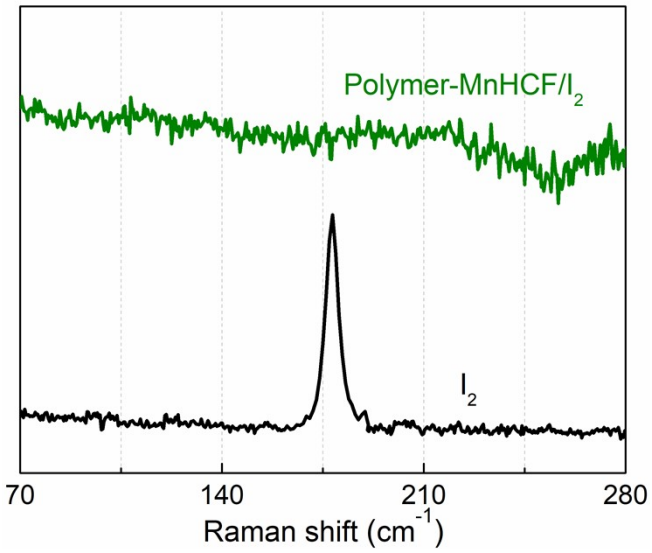

Figure S8: Raman spectrum of pure iodine and iodine loaded Polymer-MnHCF.

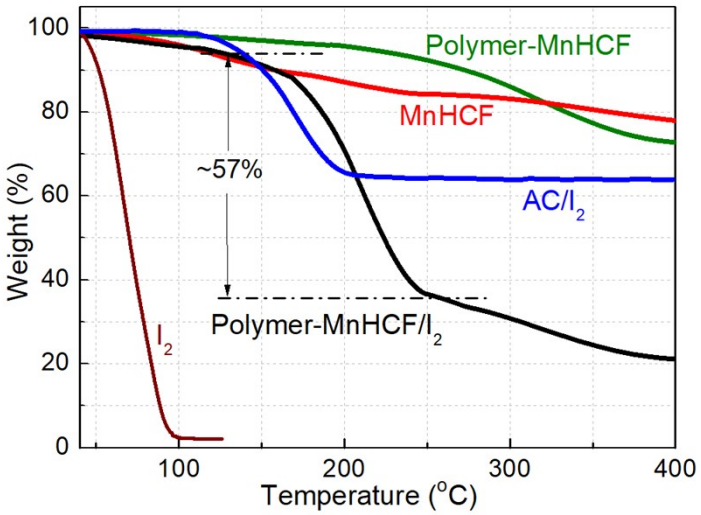

Figure S9: TGA curve of different materials.

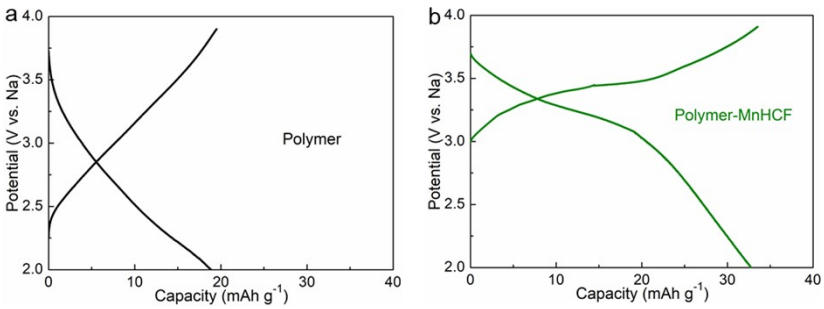

Figure S10: Charge and discharge voltage profiles (200 mA g^{-1}) of (a) Polymer and (b) Polymer-MnHCF composite host.

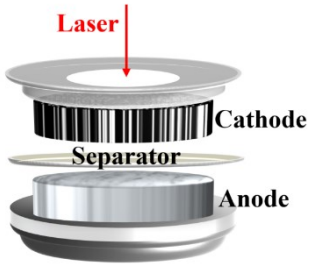

Figure S11: Schematic diagram of an in-situ Raman cell.

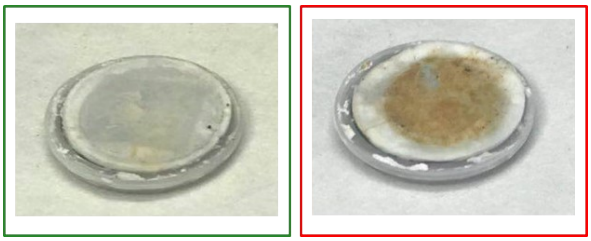

Figure S12: Digital photos of separators on cathode side (left: Polymer-MnHCF/I_2; right: Polymer/I_2) at the charged state of 3.2 V of Na-I_2 cell.

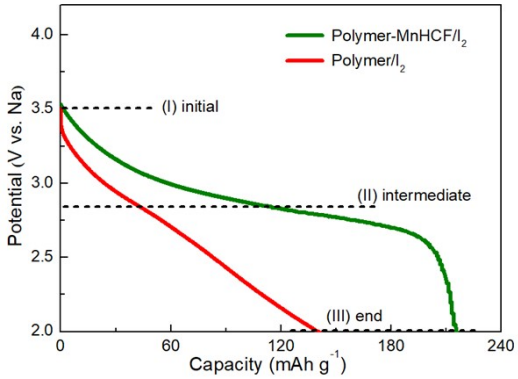

Figure S13: Discharge voltage profiles (50 mA g^{-1}) of different iodine cathodes with the same iodine loading at (I) initial, (II) intermediate and (III) end of discharge states.

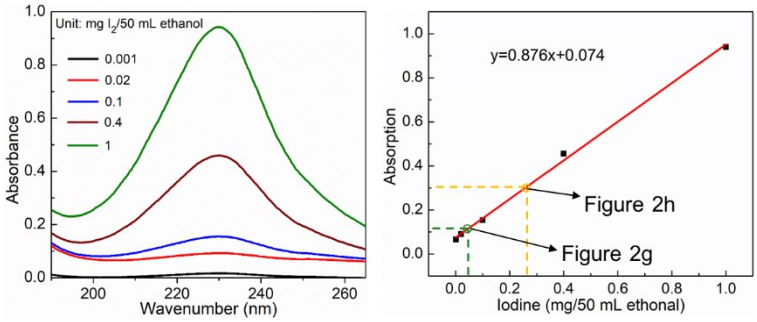

Figure S14: The typical absorption spectra of I_2 dissolved in ethanol with different concentrations. And linear relationship between the UV absorbance and the concentrations of I_2.

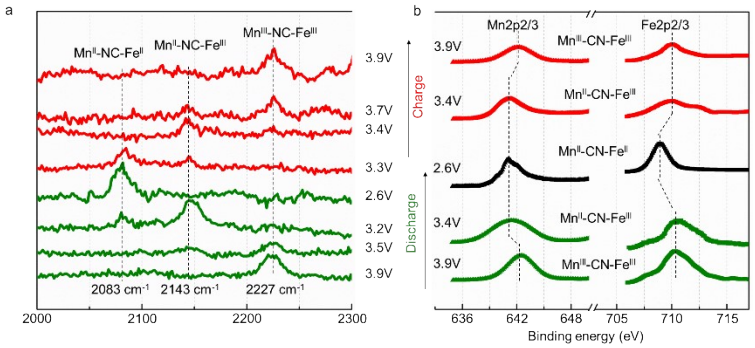

Figure S15: (a) In-situ Raman and (b) ex-situ XPS analysis of Fe-CN-Mn pair valence states of Polymer-MnHCF/I_2 cathode at different discharge and charge states.

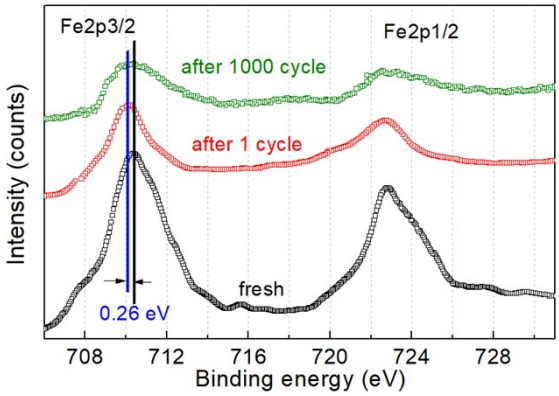

Figure S16: XPS Fe2p peaks of iodine composite cathode at fully charged state after cycling test.

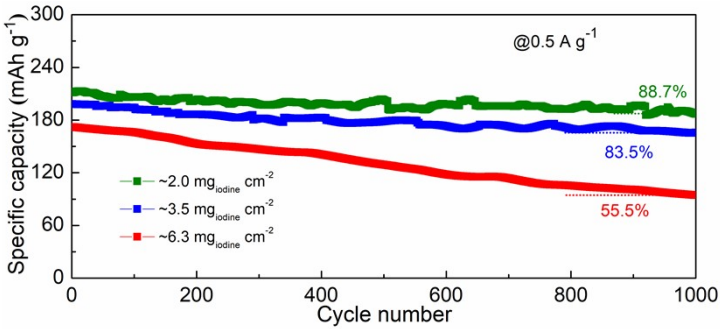

Figure S17: Cycling stability of Na-I_2 (Na-Polymer-MnHCF/I_2) cells assembled with different iodine mass loading.

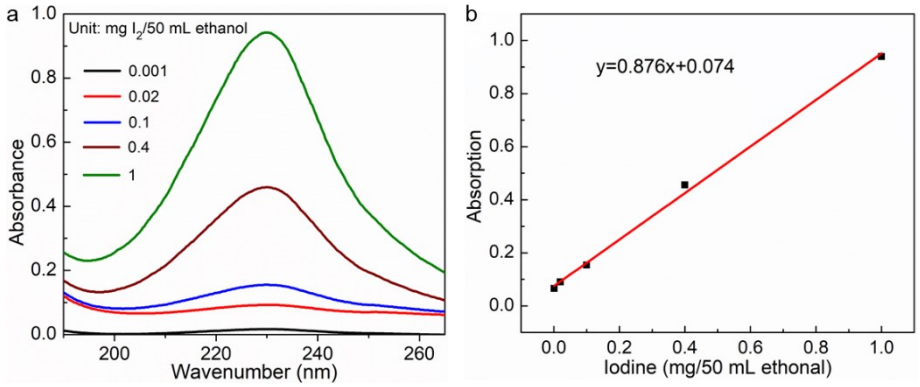

Figure S18: The typical absorption spectra of I_2 dissolved in ethanol with different concentrations; (b) The linear relationship between the UV absorbance and the concentrations of I_2. Note: To explore the iodine in composite electrode and the content of iodine in the electrolyte after cycling test, each cell was stopped at full charged state. The stainless steel coin cell and separator were washed with ethanol.

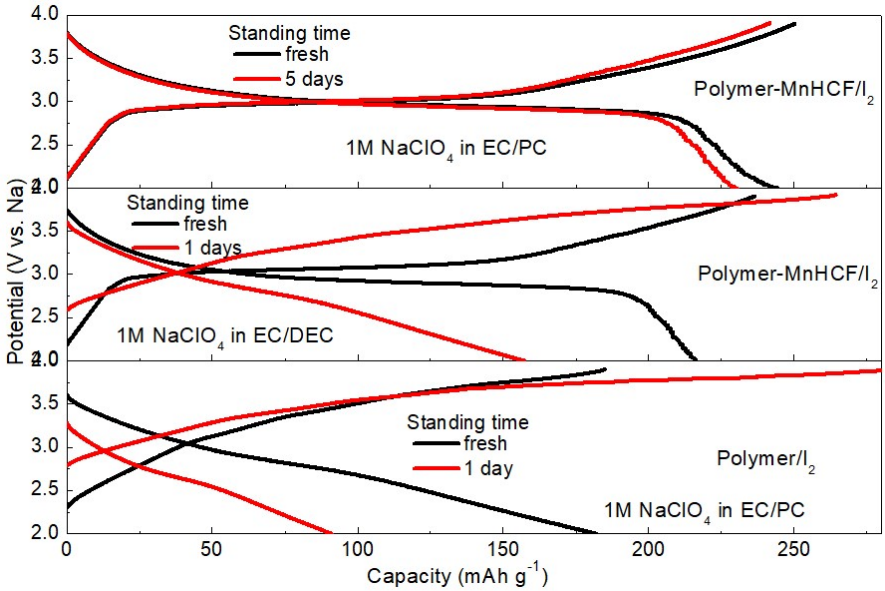

Figure S19: Discharge and charge curves of Na-iodine batteries after standing different time at current density of 200 mA/g with different iodine cathodes and electrolyte.

Table S1: Summary of BET surface area and pore volume of Polymer-MnHCF sample before and after iodine loading (50 wt%).

Sample	BET (m^2/g)	Total pore volume (cm^3/g)
Polymer-MnHCF	91	0.14
Polymer-MnHCF/I_2	9	0.02

Table S2: Summary of BET surface area of different iodine hosts.

Sample	BET (m^2/g)
Polymer-MnHCF	91

PANi-MnHCF	79
PPy-MnHCF	66
Polymer	82
MnHCF	12

Table S3. Capacity contributions of each components in the iodine composite cathode.

Electrode	Polymer-MnHCF/I_2 (2.0 mg)	[Polymer-MnHCF/I_2] I_2 (1.13 mg, 56.5 wt%)	Polymer-MnHCF (0.87 mg, 43.5 wt%)	[Polymer-MnHCF] MnHCF (0.096 mg, 11 wt%)
Capacity	0.317 mAh	0.288 mAh	0.0287 mAh	0.0117 mAh
Capacity%		90.95%	9.05%	3.69%

Table S4. Mn content in fresh and cycled samples determined by ICP-MS.

Polymer-MnHCF	Mn (wt.%)	MnHCF (wt.%)
Fresh	2.62	10.96
Cycled	2.38	9.96

Table S5. The comparison between our Polymer-MnHCF/I_2 electrode and the state-of-the-art I_2 based electrodes in Na-I_2 batteries.

Cathode (Na-I_2 cell)	Discharge capacity (mAh g^{-1})	capacity retention (current change)	Operation mechanism	Stability	Ref.
Polymer-MnHCF/I_2	**242**	**53.3%(200-5000 mA g^{-1})**	**Polyiodide-free**	**81.4%/2000cycles**	**This work**
I_2-HPCM-NP	224	62%(100-1000 mA g^{-1})	Polyiodide intermediate	85%/500cycles	Nat. Commun. 2017, 8, 527.
IQDs@RGO	170	55.9%(100-1000 mA g^{-1})	Polyiodide intermediate	82%/500cycles	Adv. Energy Mater. 2016, 1601885.
Fe_2-O_8-PcCu/I_2	208	61.5%(300-2500 mA g^{-1})	Polyiodide intermediate	95%/3200cycles	Adv. Mater. 2020, 32, 1905361.
I_2/bio-carbon	~160	~	Polyiodide intermediate	91%/500cycles	Nanoscale 2017, 9, 9365.
polymer@carbon-I_2	~210	33%(0.5-20 C)	Polyiodide intermediate	73%/400cycles	J. Mater. Chem. A 2018, 6, 9019.
ACC/I_2	229.5	30.6%(0.1-5 C)	Polyiodide intermediate	short circuiting/750cycles	Nano Energy 2019, 57, 692.

Referenece

1. Pan, H.; Shao, Y.; Yan, P.; Cheng, Y.; Han, K. S.; Nie, Z.; Wang, C.; Yang, J.; Li, X.; Bhattacharya, P.; Mueller, K. T.; Liu, J., Reversible aqueous zinc/manganese oxide energy storage from conversion reactions. *Nat. Energy* **2016**, *1*, 16039.
2. Zhang, J.; Shi, Y.; Ding, Y.; Zhang, W.; Yu, G. In Situ Reactive Synthesis of Polypyrrole-MnO_2 Coaxial Nanotubes as Sulfur Hosts for High-Performance Lithium-Sulfur Battery. *Nano Lett*. **2016**, *16*, 7276-7281.
3. Lu, K.; Hu, Z.; Ma, J.; Ma, H.; Dai, L.; Zhang, J. A rechargeable iodine-carbon battery that exploits ion intercalation and iodine redox chemistry. *Nat*. *Commun*. **2017**, *8*, 1-10.